

# Quantile autoregressive moving average models for ratio-based bounded time series

Helton Saulo<sup>\*1,2</sup>, Roberto Vila<sup>†1</sup>, and Filidor Vilca<sup>‡3</sup>

<sup>1</sup>*Department of Statistics, University of Brasília, Brasília, Brazil*

<sup>2</sup>*Department of Economics, Federal University of Pelotas, Pelotas, Brazil*

<sup>2</sup>*Department of Statistics, State University of Campinas, Campinas, Brazil*

May 26, 2026

## Abstract

This paper proposes the quantile unit-log-symmetric autoregressive moving average (QULS–ARMA) model for bounded time series on the open unit interval  $(0, 1)$ . The model extends the unit-log-symmetric family by introducing a quantile-based reparameterization and embedding autoregressive and moving-average dynamics directly in the conditional quantile, thereby overcoming limitations of mean-based approaches and providing a coherent framework for proportion data arising from ratios of dependent positive variables. The proposed specification accommodates asymmetric behavior and heavy tails through flexible log-symmetric kernels, including the normal and Student- $t$  distributions. Parameter estimation is carried out via conditional maximum likelihood, and asymptotic properties are established. Monte Carlo simulations and an empirical application to hydroelectric energy storage proportions in Brazil assess the finite-sample performance and practical advantages of the QULS–ARMA model. The results show the good performance of the proposed estimators across a range of scenarios and kernel specifications.

**Keywords.** Unit-log-symmetric distribution · ARMA models · Bounded distributions · Monte Carlo simulation · Proportion data

**Mathematics Subject Classification (2010).** MSC 60E05 · MSC 62Exx · MSC 62Fxx.

---

\*Corresponding author: [heltonsaulo@gmail.com](mailto:heltonsaulo@gmail.com)

†[rovig161@gmail.com](mailto:rovig161@gmail.com)

‡[fily@unicamp.br](mailto:fily@unicamp.br)

# 1 Introduction

Bounded time series data, such as rates and proportions, commonly arise in a wide range of applications in economics, finance, biology, and environmental sciences. Typical examples include market shares, default probabilities, employment ratios, and energy use fractions. Modeling such data is challenging because standard time series models defined on the real line may yield predictions outside the unit interval  $(0, 1)$ . As a result, several bounded autoregressive moving average (ARMA) frameworks have been developed in recent years, most notably those based on the beta distribution (Ferrari and Cribari-Neto, 2004; Rocha and Cribari-Neto, 2009) and the Kumaraswamy distribution (Kumaraswamy, 1980; Bayer et al., 2017), which typically model the conditional mean. More recently, Ribeiro et al. (2023) proposed a unit Burr XII quantile autoregressive moving average (UBXII-ARMA) model, extending static unit distributions to dynamic frameworks through ARMA-type dynamics on conditional quantiles.

Despite their flexibility, those existing methodologies for bounded time series present important conceptual limitations when applied to asymmetric proportion data. In particular, the beta and Kumaraswamy ARMA-type models are formulated in terms of the conditional mean, which may be an inadequate central tendency measure when the distribution is skewed. Quantile-based approaches partially address this issue by modeling the conditional quantiles directly. A notable example is the UBXII-ARMA model proposed by Ribeiro et al. (2023), which introduces ARMA-type dynamics in the conditional quantile of a unit Burr XII distribution. Although this framework represents a substantial advance over mean-based models, its probabilistic construction is not explicitly linked to a ratio-type data-generating mechanism. As a consequence, the underlying stochastic structure does not directly reflect situations in which the observed proportion arises from dependent random variables.

An alternative and conceptually appealing approach for modeling bounded data is based on log-symmetric distributions (Vanegas and Paula, 2016). This class generalizes the log-normal distribution by allowing the underlying symmetric kernel to belong to families such as the normal or Student- $t$ , thereby accommodating different tail behaviors and degrees of robustness. Extending this idea, Vila et al. (2023) introduced the bivariate log-symmetric (BLS) distribution to model possibly correlated positive random variables. Building on this construction, Vila et al. (2024) proposed the unit-log-symmetric (ULS) distribution, obtained through the transformation

$$W = \frac{T_1}{T_1 + T_2},$$

where  $(T_1, T_2)$  follows a bivariate log-symmetric distribution. This formulation provides a natural probabilistic foundation for proportion data arising from ratios of positive quantities.

In many applied settings, such as the proportion of stored hydroelectric energy, the observed bounded series is naturally expressed as a ratio of latent positive quantities evolving over time. Ignoring this structural feature may limit interpretability and coherence between the assumed distribution and the physical mechanism generating the data. These considerations highlight the need for dynamic quantile models that simultaneously (i) accommodate asymmetry through conditional quantiles, (ii) capture serial dependence, and (iii) are grounded on a ratio-based probabilistic construction.

However, to the best of our knowledge, no work has simultaneously combined a ratio-based bounded distribution with ARMA-type dynamics on conditional quantiles. Motivated by these developments, the main objective of this paper is to propose the quantile unit-log-symmetric autoregressive moving average (QULS–ARMA) model, a new class of dynamic models for bounded time series. Secondary objectives are to (a) introduce a quantile reparameterization of the ULS distribution, yielding the QULS distribution; (b) develop conditional maximum likelihood estimation and establish asymptotic properties of the resulting estimators; and (c) illustrate the finite-sample performance of the proposed estimators through Monte Carlo simulations and an empirical application to hydroelectric energy storage proportions.

The rest of this paper proceeds as follows. In Section 2, we briefly provide a motivation example. In Section 3, we describe the usual ULS distribution and propose a reparameterization of this distribution in terms of a quantile parameter. In Section 4, we introduce the QULS–ARMA model, presenting its probabilistic construction, dynamic specification, and main properties. In this section, we also describe the parameter estimation procedure based on conditional maximum likelihood and discuss inferential aspects. In Section 5, we report a Monte Carlo simulation study assessing the finite-sample performance of the proposed estimators under different scenarios. In Section 6, an empirical application to monthly proportions of stored hydroelectric energy in Brazil is presented, where the proposed model is compared with existing alternatives in terms of in-sample fit and out-of-sample forecasting. Finally, in Section 7, we provide some concluding remarks.

## 2 Motivating example and modeling rationale

Bounded time series frequently arise in applications where the variable of interest is naturally expressed as a proportion or ratio. A particularly relevant example in energy economics and hydrology is the monthly proportion of stored hydroelectric energy (Bayer et al., 2017), which can be interpreted as the ratio between the current volume of stored water and the total storage capacity of the system. Formally, if  $T_{1,t}$  denotes the effective stored water volume at time  $t$  and  $T_{2,t}$  the remaining or complementary capacity, the observed proportion may be written as

$$Y_t = \frac{T_{1,t}}{T_{1,t} + T_{2,t}}, \quad 0 < Y_t < 1.$$

This representation naturally motivates probability models derived from ratios of positive random variables, rather than ad hoc bounded distributions.

From a physical and operational perspective, the components  $T_{1,t}$  and  $T_{2,t}$  are intrinsically linked through the following mechanism: increases in stored volume necessarily reduce the available remaining capacity, inducing a negative association between these quantities. Existing approaches for bounded time series, such as beta, Kumaraswamy and unit Burr XII autoregressive models, incorporate temporal dependence through the conditional mean or conditional quantiles, but they do not explicitly reflect the ratio-based structure suggested by the underlying data-generating mechanism. In contrast, the ULS distribution arises directly from ratios

of log-symmetric random variables, providing a more coherent and interpretable probabilistic foundation for proportion data. It is on this foundation that the proposed QULS–ARMA model is built, extending the ULS distribution to a dynamic framework by allowing autoregressive and moving-average dependence in the conditional quantile.

### 3 Reparameterized unit-log-symmetric distribution by the quantile

A continuous random variable  $Y$  with support  $(0, 1)$  is said to follow a unit-log-symmetric (ULS) distribution with parameters  $\eta > 0$  and  $\sigma > 0$ , denoted by  $Y \sim \text{ULS}(\eta, \sigma)$ , if its probability density function (PDF) is given by

$$f_Y(y; \eta, \sigma) = \frac{1}{\sigma y(1-y)} f_Z\left(\frac{1}{\sigma} \log\left[\frac{y}{\eta(1-y)}\right]\right), \quad 0 < y < 1, \quad (3.1)$$

where  $f_Z(\cdot)$  denotes the PDF of a standard symmetric random variable  $Z$  on the real line, typically following a normal or Student- $t$  distribution.

The corresponding cumulative distribution function (CDF) is

$$F_Y(y; \eta, \sigma) = F_Z\left(\frac{1}{\sigma} \log\left[\frac{y}{\eta(1-y)}\right]\right), \quad 0 < y < 1, \quad (3.2)$$

where  $F_Z(\cdot)$  is the CDF of  $Z$ .

This transformation maps  $(0, 1)$  onto  $\mathbb{R}$  through

$$z = \frac{1}{\sigma} \log\left(\frac{y}{\eta(1-y)}\right),$$

ensuring that  $f_Y(y; \eta, \sigma)$  is a valid PDF for all  $y \in (0, 1)$ . The parameters  $\eta$  and  $\sigma$  govern, respectively, the location (through a logit-type shift) and the dispersion of the distribution on the unit interval.

Let  $Q_Z(\tau)$  be the  $\tau$ -th quantile of the base distribution  $Z$ . From (3.2), the quantile function of  $Y$  is given by

$$q_\tau = \frac{\eta \exp(\sigma Q_Z(\tau))}{1 + \eta \exp(\sigma Q_Z(\tau))}, \quad 0 < \tau < 1. \quad (3.3)$$

This ensures  $q_\tau \in (0, 1)$  for all admissible parameters and provides an explicit link between the quantiles of  $Z$  and  $Y$ .

Solving (3.3) for  $\eta$ , we obtain

$$\eta = \frac{q_\tau}{1 - q_\tau} \exp[-\sigma Q_Z(\tau)], \quad (3.4)$$

yielding a one-to-one mapping between  $(\eta, \sigma)$  and  $(q_\tau, \sigma)$  for a fixed quantile level  $\tau$ . Hence, we can reparameterize the ULS model in terms of the quantile parameter  $q_\tau$  instead of  $\eta$ . By substituting (3.4) into (3.1), the PDF of  $Y$  under the quantile reparameterization becomes

$$f_Y(y; q_\tau, \sigma) = \frac{1}{\sigma y(1-y)} f_Z\left(\frac{1}{\sigma} \log\left[\frac{y(1-q_\tau) \exp(\sigma Q_Z(\tau))}{q_\tau(1-y)}\right]\right), \quad 0 < y < 1. \quad (3.5)$$

The notation  $Y \sim \text{ULS}(q_\tau, \sigma)$  is used.

## 4 Quantile unit-log-symmetric ARMA models

### 4.1 The model

Let  $\{Y_t\}_{t=1}^n$  be a sequence of random variables defined on the probability space  $(\Omega, \mathcal{A}, \mathbb{P})$  and, for each  $t \geq 1$ , let

$$\mathcal{A}_t = \sigma(Y_1, \dots, Y_t) = \sigma\left(\{\cap_{i=1}^k Y_i^{-1}(B_i) : B_1, \dots, B_k \text{ Borel sets in } \mathbb{R}, k = 1, \dots, t\}\right)$$

be the  $\sigma$ -algebra generated by the information available up to time  $t$ , with  $\mathcal{A}_0 = \{\Omega, \emptyset\}$ . Fix a quantile level  $\tau \in (0, 1)$  and let  $Q_Z(\tau)$  denote the  $\tau$ -th quantile of a symmetric kernel  $Z$  on  $\mathbb{R}$  (e.g., Normal or Student- $t$ ). Assume that the conditional distribution of  $Y_t$  given  $\mathcal{A}_{t-1}$  is unit-log-symmetric, parameterized by its  $\tau$ -th conditional quantile  $q_{\tau,t} \in (0, 1)$  and a scale  $\sigma > 0$ :

$$Y_t \mid \mathcal{A}_{t-1} \sim \text{ULS}(q_{\tau,t}, \sigma).$$

Then, the conditional PDF of  $Y_t \mid \mathcal{A}_{t-1}$  is

$$f_{Y_t \mid \mathcal{A}_{t-1}}(y_t; q_{\tau,t}, \sigma) = \frac{1}{\sigma y_t(1-y_t)} f_Z\left(\frac{1}{\sigma} \log\left[\frac{y_t(1-q_{\tau,t}) \exp\{\sigma Q_Z(\tau)\}}{q_{\tau,t}(1-y_t)}\right]\right), \quad 0 < y_t < 1, \quad (4.1)$$

where  $f_Z$  is the density of the symmetric kernel  $Z$  and  $Q_Z(\tau)$  is treated as known for the chosen kernel and  $\tau$ .

Let  $g : (0, 1) \rightarrow \mathbb{R}$  be a strictly increasing, twice continuously differentiable link (e.g., logit, probit, complementary log-log), with inverse  $g^{-1}$ . Define the linked conditional quantile

$$\eta_t = g(q_{\tau,t}),$$

and the innovation on the link scale

$$r_t := g(Y_t) - g(q_{\tau,t}).$$

Because  $g$  is monotone, the conditional  $\tau$ -quantile commutes with  $g$ , hence

$$\mathbb{P}(r_t \leq 0 \mid \mathcal{A}_{t-1}) = \mathbb{P}(g(Y_t) \leq g(q_{\tau,t}) \mid \mathcal{A}_{t-1}) = \tau, \quad \text{so} \quad Q_{r_t \mid \mathcal{A}_{t-1}}(\tau) = 0 \quad \text{a.s.}$$

Let  $\mathbf{x}_t = (1, x_{t1}, \dots, x_{tk})^\top$  collect exogenous covariates ( $k < n$ ). We specify

$$\eta_t = g(q_{\tau,t}) = \alpha + \mathbf{x}_t^\top \boldsymbol{\beta} + \varrho_t, \quad t = m+1, \dots, n, \quad (4.2)$$

with  $m = \max\{p, q\}$  and  $\boldsymbol{\beta} = (\beta_1, \dots, \beta_k)^\top$ , whereas the dynamic component  $\varrho_t$  follows the ARMA scheme

$$\varrho_t = \alpha + \sum_{i=1}^p \phi_i \left[ g(Y_{t-i}) - \mathbf{x}_{t-i}^\top \boldsymbol{\beta} \right] + \sum_{j=1}^q \theta_j r_{t-j}, \quad Q_{r_t | \mathcal{A}_{t-1}}(\tau) = 0 \text{ a.s.}, \quad (4.3)$$

where  $\boldsymbol{\phi} = (\phi_1, \dots, \phi_p)^\top$  and  $\boldsymbol{\theta} = (\theta_1, \dots, \theta_q)^\top$  are the autoregressive and moving-average parameter vectors, respectively. Combining (4.2)–(4.3) yields

$$g(q_{\tau,t}) = \alpha + \mathbf{x}_t^\top \boldsymbol{\beta} + \sum_{i=1}^p \phi_i \left[ g(Y_{t-i}) - \mathbf{x}_{t-i}^\top \boldsymbol{\beta} \right] + \sum_{j=1}^q \theta_j r_{t-j}, \quad Q_{r_t | \mathcal{A}_{t-1}}(\tau) = 0. \quad (4.4)$$

Since  $g(Y_t) = g(q_{\tau,t}) + r_t$ , equations (4.2) and (4.4) imply

$$g(Y_t) = \alpha + \mathbf{x}_t^\top \boldsymbol{\beta} + \sum_{i=1}^p \phi_i \left[ g(Y_{t-i}) - \mathbf{x}_{t-i}^\top \boldsymbol{\beta} \right] + \sum_{j=1}^q \theta_j r_{t-j} + r_t, \quad Q_{r_t | \mathcal{A}_{t-1}}(\tau) = 0. \quad (4.5)$$

Equation (4.5) defines the QULS–ARMA( $p, q$ ) model on the link scale.

Let  $L$  denote the lag operator ( $L^k X_t = X_{t-k}$ ) and define the polynomials

$$\Phi(L) = 1 - \sum_{i=1}^p \phi_i L^i, \quad \Theta(L) = 1 + \sum_{j=1}^q \theta_j L^j.$$

Then (4.5) can be written compactly as

$$\Phi(L) \left[ g(Y_t) - \mathbf{x}_t^\top \boldsymbol{\beta} \right] = \Theta(L) r_t, \quad Q_{r_t | \mathcal{A}_{t-1}}(\tau) = 0. \quad (4.6)$$

## 4.2 Estimation and inference

Estimation of the parameters of the ULS–ARMA( $p, q$ ) model is carried out through conditional maximum likelihood (CML), using the first  $m = \max\{p, q\}$  observations to initialize the recursion. Let

$$\boldsymbol{\vartheta} = (\vartheta : \vartheta \in \{\alpha, \beta_1, \dots, \beta_k, \sigma, \phi_1, \dots, \phi_p, \theta_1, \dots, \theta_q\})^\top = (\alpha, \boldsymbol{\beta}^\top, \sigma, \boldsymbol{\phi}^\top, \boldsymbol{\theta}^\top)^\top$$

denote the full parameter vector, where  $\boldsymbol{\beta}$  is the regression coefficient vector,  $\sigma > 0$  the scale parameter of the ULS distribution, and  $\boldsymbol{\phi}$  and  $\boldsymbol{\theta}$  collect the autoregressive and moving-average parameters, respectively.

Given the conditional density  $f_{Y_t|\mathcal{A}_{t-1}}(y_t; q_{\tau,t}, \sigma)$  in (4.1), the conditional likelihood based on the sample  $\{y_{m+1}, \dots, y_n\}$  is

$$L(\boldsymbol{\vartheta})_{m,n} = \prod_{t=m+1}^n f_{Y_t|\mathcal{A}_{t-1}}(y_t; q_{\tau,t}(\boldsymbol{\vartheta}), \sigma), \quad 0 < y_t < 1,$$

which leads to the conditional log-likelihood (up to an additive constant)

$$\ell(\boldsymbol{\vartheta})_{m,n} = - \sum_{t=m+1}^n \log(\sigma y_t(1-y_t)) + \sum_{t=m+1}^n \log f_Z \left( \frac{1}{\sigma} \log \left[ \frac{y_t(1-q_{\tau,t}) \exp\{\sigma Q_Z(\tau)\}}{q_{\tau,t}(1-y_t)} \right] \right), \quad (4.7)$$

where  $f_Z$  and  $Q_Z(\tau)$  are, respectively, the density and  $\tau$ -quantile of the chosen symmetric kernel  $Z$  (e.g., normal, Student- $t$ ). Maximization of (4.7) is performed numerically. The score vector  $\dot{\ell}(\boldsymbol{\vartheta})$  is obtained by differentiation of  $\ell(\boldsymbol{\vartheta})_{m,n}$  with respect to each component of  $\boldsymbol{\vartheta}$ , and the resulting likelihood equations are solved through iterative methods such as the Broyden-Fletcher-Goldfarb-Shanno (BFGS) algorithm. The components of the score vector  $\dot{\ell}(\boldsymbol{\vartheta})$  are given by

$$\frac{\partial \ell(\boldsymbol{\vartheta})_{m,n}}{\partial \vartheta} = - \frac{(n-m)}{\sigma} \delta_{\vartheta, \sigma} + \sum_{t=m+1}^n \frac{f'_Z(w_t)}{f_Z(w_t)} \frac{\partial w_t}{\partial \vartheta}, \quad \vartheta \in \{\alpha, \beta_1, \dots, \beta_k, \sigma, \phi_1, \dots, \phi_p, \theta_1, \dots, \theta_q\},$$

where  $\delta_{x,y}$  is the dirac delta function and

$$w_t \equiv \frac{1}{\sigma} \log \left[ \frac{y_t(1-q_{\tau,t}) \exp\{\sigma Q_Z(\tau)\}}{q_{\tau,t}(1-y_t)} \right].$$

Furthermore,

$$\frac{\partial w_t}{\partial \vartheta} = - \frac{1}{\sigma} \frac{1}{(1-q_{\tau,t})q_{\tau,t}} \frac{\partial q_{\tau,t}}{\partial \vartheta}, \quad \vartheta \in \{\alpha, \beta_1, \dots, \beta_k, \phi_1, \dots, \phi_p, \theta_1, \dots, \theta_q\}, \quad (4.8)$$

$$\frac{\partial w_t}{\partial \sigma} = - \frac{1}{\sigma^2} \log \left[ \frac{y_t(1-q_{\tau,t})}{q_{\tau,t}(1-y_t)} \right], \quad (4.9)$$

and, by using (4.4),

$$\frac{\partial q_{\tau,t}}{\partial \alpha} = \frac{1}{g'(q_{\tau,t})} \left[ 1 - \sum_{i=1}^p \phi_i \right], \quad (4.10)$$

$$\frac{\partial q_{\tau,t}}{\partial \beta_l} = \frac{1}{g'(q_{\tau,t})} \left[ x_{tl} - \sum_{i=1}^p \phi_i x_{(t-i)l} \right], \quad l = 1, \dots, k, \quad (4.11)$$

$$\frac{\partial q_{\tau,t}}{\partial \phi_u} = \frac{1}{g'(q_{\tau,t})} \left[ g(Y_{t-u}) - \mathbf{x}_{t-u}^\top \boldsymbol{\beta} \right], \quad u = 1, \dots, p, \quad (4.12)$$

$$\frac{\partial q_{\tau,t}}{\partial \theta_v} = \frac{1}{g'(q_{\tau,t})} \theta_v r_{t-v}, \quad v = 1, \dots, q. \quad (4.13)$$

Appropriate starting values are required to initialize the optimization routine; these may be derived from least-squares-type estimators for the ARMA structure or from standard R functions such as `arima`, combined with preliminary estimates of  $\sigma$  from ULS models.

In (4.7), when the symmetric kernel is taken to be Student- $t$ , the model includes an additional degrees-of-freedom parameter, denoted by  $\nu$ . Following Lucas (1997), we do not estimate  $\nu$  jointly with the remaining parameters. As argued in Lucas (1997), the desirable robustness properties of the Student- $t$  specification are preserved only when  $\nu$  is treated as fixed rather than estimated by maximum likelihood. Therefore, the estimation of  $\boldsymbol{\vartheta}$  proceeds in two stages for the Student- $t$  case. *Step 1:* Select a grid of candidate values for  $\nu$ ,  $\nu_1, \nu_2, \dots, \nu_K$ , and for each fixed  $\nu_i$  maximize the conditional likelihood with respect to the remaining parameters, obtaining the corresponding log-likelihood value. *Step 2:* Choose the value of  $\nu_i$  that yields the highest log-likelihood, and adopt the associated parameter estimates as the final CML estimates.

Under the usual regularity conditions for conditional likelihood estimation (Assumptions 2.1–2.5 in Andersen 1970) and assuming  $n$  sufficiently large, the CML estimator  $\hat{\boldsymbol{\vartheta}}$  is asymptotically normal:

$$\sqrt{n}(\hat{\boldsymbol{\vartheta}} - \boldsymbol{\vartheta}) \xrightarrow{\mathcal{D}} N_d(\mathbf{0}, \mathcal{I}(\boldsymbol{\vartheta})^{-1}), \quad n \rightarrow \infty,$$

where  $d$  is the dimension of  $\boldsymbol{\vartheta}$  and  $\mathcal{I}(\boldsymbol{\vartheta})$  is the Fisher information matrix. In applications,  $\mathcal{I}(\boldsymbol{\vartheta})$  is commonly approximated by the inverse of the observed information matrix, obtained from the negative Hessian  $\mathcal{J}(\boldsymbol{\vartheta}) = -\partial^2 \ell(\boldsymbol{\vartheta})_{m,n} / \partial \boldsymbol{\vartheta} \partial \boldsymbol{\vartheta}^\top$  evaluated at  $\hat{\boldsymbol{\vartheta}}$ . The elements of the Hessian matrix  $\partial^2 \ell(\boldsymbol{\vartheta})_{m,n} / \partial \boldsymbol{\vartheta} \partial \boldsymbol{\vartheta}^\top$  are given by

$$\frac{\partial^2 \ell(\boldsymbol{\vartheta})_{m,n}}{\partial \vartheta \partial \tilde{\vartheta}} = \frac{(n-m)}{\sigma^2} \delta_{\vartheta, \sigma} \delta_{\tilde{\vartheta}, \sigma} + \sum_{t=m+1}^n \left[ \frac{f_Z''(w_t) f_Z(w_t) - \{f_Z'(w_t)\}^2}{\{f_Z(w_t)\}^2} \frac{\partial w_t}{\partial \vartheta} \frac{\partial w_t}{\partial \tilde{\vartheta}} + \frac{f_Z'(w_t)}{f_Z(w_t)} \frac{\partial^2 w_t}{\partial \vartheta \partial \tilde{\vartheta}} \right],$$

where

$$\vartheta, \tilde{\vartheta} \in \{\alpha, \beta_1, \dots, \beta_k, \sigma, \phi_1, \dots, \phi_p, \theta_1, \dots, \theta_q\},$$

and  $\partial w_t / \partial \vartheta$  and  $\partial w_t / \partial \tilde{\vartheta}$  are given in (4.8)-(4.9). Moreover,

$$\frac{\partial w_t}{\partial \vartheta} = \frac{1}{\sigma} \frac{1}{(1 - q_{\tau,t}) q_{\tau,t}} \left[ \frac{(1 - 2q_{\tau,t})}{(1 - q_{\tau,t}) q_{\tau,t}} \frac{\partial q_{\tau,t}}{\partial \vartheta} \frac{\partial q_{\tau,t}}{\partial \tilde{\vartheta}} - \frac{\partial^2 q_{\tau,t}}{\partial \vartheta \partial \tilde{\vartheta}} \right], \quad \vartheta, \tilde{\vartheta} \in \{\alpha, \beta_1, \dots, \beta_k, \phi_1, \dots, \phi_p, \theta_1, \dots, \theta_q\},$$

$$\frac{\partial w_t}{\partial \sigma} = \frac{2}{\sigma^3} \log \left[ \frac{y_t (1 - q_{\tau,t})}{q_{\tau,t} (1 - y_t)} \right],$$

where  $\partial q_{\tau,t} / \partial \vartheta$  and  $\partial q_{\tau,t} / \partial \tilde{\vartheta}$  are given in (4.10)-(4.13), and  $\partial^2 q_{\tau,t} / \partial \vartheta \partial \tilde{\vartheta}$  can be readily derived through routine calculations from (4.10)-(4.13).

The quantile level  $\tau$  is chosen by the practitioner according to the purpose of the analysis, and the selected  $\tau$  determines the conditional quantile tracked by the ULS-ARMA model. Regarding the link  $g(\cdot)$ , common options include the logit, probit, and complementary log-log functions. Model selection can be guided by information criteria such as AIC or BIC. The logit link is particularly attractive because it ensures that  $q_{\tau,t} \in (0, 1)$  for all  $t$ .

As in other quantile-based time series frameworks, if several quantiles are modeled independently, their estimated trajectories might not satisfy the natural monotonicity across  $\tau$ . Hence, care must be exercised when interpreting multiple-quantile ULS–ARMA fits, as pointed out by [Koenker and Xiao \(2006\)](#) in the broader context of quantile regression.

### 4.3 Prediction

After obtaining the conditional maximum likelihood estimates of the parameters in the ULS–ARMA( $p, q$ ) model, we now describe the procedure for generating forecasts of the bounded time series  $\{Y_t\}$ . Let  $\hat{Y}_{t+h}$  denote the  $h$ -step-ahead prediction based on the information set  $\mathcal{A}_t$ . For notational convenience, we set

$$\hat{Y}_{t+h} = \begin{cases} \hat{Y}_t(h), & h > 0, \\ Y_{t+h}, & h \leq 0, \end{cases} \quad \text{and} \quad \hat{r}_{t+h} = \begin{cases} 0, & h > 0, \\ \hat{r}_{t+h}, & h \leq 0, \end{cases}$$

reflecting the fact that future innovations on the link scale have conditional  $\tau$ -quantile equal to zero. The conditional quantile is determined through the link function  $g : (0, 1) \rightarrow \mathbb{R}$  and the ARMA structure imposed on  $g(q_{\tau,t})$ . Given the estimated parameters  $\hat{\boldsymbol{\beta}}, \hat{\phi}_1, \dots, \hat{\phi}_p$  and  $\hat{\theta}_1, \dots, \hat{\theta}_q$ , the fitted conditional  $\tau$ -quantile at time  $t$  is

$$\hat{\eta}_t = g(\hat{q}_{\tau,t}) = \hat{\alpha} + \mathbf{x}_t^\top \hat{\boldsymbol{\beta}} + \sum_{i=1}^p \hat{\phi}_i [g(Y_{t-i}) - \mathbf{x}_{t-i}^\top \hat{\boldsymbol{\beta}}] + \sum_{j=1}^q \hat{\theta}_j \hat{r}_{t-j}. \quad (4.14)$$

Since the innovation on the link scale satisfies

$$r_t = g(Y_t) - g(q_{\tau,t}),$$

an empirical estimate is obtained from the fitted model as

$$\hat{r}_t = g(Y_t) - \hat{\eta}_t, \quad t = m+1, \dots, n,$$

which justifies the convention  $\hat{r}_{t+h} = 0$  for  $h > 0$ .

Using (4.14), the one-step-ahead forecast is given by

$$\hat{Y}_{n+1} = g^{-1} \left( \hat{\alpha} + \mathbf{x}_{n+1}^\top \hat{\boldsymbol{\beta}} + \sum_{i=1}^p \hat{\phi}_i [g(Y_{n+1-i}) - \mathbf{x}_{n+1-i}^\top \hat{\boldsymbol{\beta}}] + \sum_{j=1}^q \hat{\theta}_j \hat{r}_{n+1-j} \right). \quad (4.15)$$

The same reasoning yields the forecast for time  $n+2$ :

$$\hat{Y}_{n+2} = g^{-1} \left( \hat{\alpha} + \mathbf{x}_{n+2}^\top \hat{\boldsymbol{\beta}} + \sum_{i=1}^p \hat{\phi}_i [g(\hat{Y}_{n+2-i}) - \mathbf{x}_{n+2-i}^\top \hat{\boldsymbol{\beta}}] + \sum_{j=1}^q \hat{\theta}_j \hat{r}_{n+2-j} \right),$$

where all terms involving future values are replaced by their corresponding forecasts. The recursion extends naturally to any horizon  $h > 2$ .

## 5 Monte Carlo simulation study

This section reports a Monte Carlo study assessing the finite-sample performance of the conditional maximum likelihood (CML) estimators in the proposed ULS–ARMA framework under the normal kernel. The objective is to assess bias, relative bias, absolute relative bias, and root mean squared error of the estimators across different dependence structures, dispersion levels, and quantile levels  $\tau \in \{0.25, 0.50, 0.75\}$ .

### 5.1 Data generating process

Let  $\{Y_t\}_{t \geq 1}$  be a bounded time series with  $Y_t \in (0, 1)$ . Fix a quantile level  $\tau \in (0, 1)$  and define the linked conditional quantile  $\eta_t = g(q_{\tau,t})$  with  $g(\cdot)$  the logit link,  $g(u) = \log\{u/(1-u)\}$ . Under the ULS–ARMA( $p, q$ ) model,

$$\eta_t = \alpha + \mathbf{x}_t^\top \boldsymbol{\beta} + \sum_{i=1}^p \phi_i \left( g(Y_{t-i}) - \mathbf{x}_{t-i}^\top \boldsymbol{\beta} \right) + \sum_{j=1}^q \theta_j r_{t-j}, \quad t > m, \quad (5.1)$$

where  $m = \max\{p, q\}$ ,  $\boldsymbol{\beta} = (\beta_1, \beta_2)^\top$ , and the innovation on the link scale is  $r_t = g(Y_t) - \eta_t$ . The conditional distribution is assumed to be unit-log-symmetric,

$$Y_t \mid \mathcal{A}_{t-1} \sim \text{ULS}(q_{\tau,t}, \sigma; \text{kernel}), \quad q_{\tau,t} = g^{-1}(\eta_t), \quad \sigma > 0, \quad (5.2)$$

where “kernel” stands for Normal(0, 1).

In order to simulate from (5.2) under the quantile parameterization, we exploit the explicit stochastic representation induced by the logit transformation. Let  $Z_t$  be drawn independently from the chosen kernel with  $\tau$ -th quantile  $Q_Z(\tau)$ . Then

$$Y_t = g^{-1} \left( \eta_t + \sigma \{Z_t - Q_Z(\tau)\} \right), \quad (5.3)$$

which ensures that the conditional  $\tau$ -quantile of  $Y_t$  given  $\mathcal{A}_{t-1}$  is exactly  $q_{\tau,t}$ , since  $\mathbb{P}(Z_t \leq Q_Z(\tau)) = \tau$  by construction. For the normal kernel,  $Q_Z(\tau) = \Phi^{-1}(\tau)$ . The simulated innovation  $r_t$  follows immediately as  $r_t = g(Y_t) - \eta_t$ . We consider three quantile levels,  $\tau \in \{0.25, 0.50, 0.75\}$ , in order to assess the finite-sample performance of the CML estimators across the lower quartile, the conditional median, and the upper quartile of the conditional distribution.

We adopt a parsimonious harmonic specification to generate deterministic covariates,

$$\mathbf{x}_t = \left( \cos(2\pi t/12), \sin(2\pi t/12) \right)^\top,$$

so that  $\mathbf{x}_t^\top \boldsymbol{\beta}$  acts as a seasonal component on the link scale. This is aligned with the empirical application, where harmonic terms capture annual periodicity. We consider four scenarios combining different dynamic orders and dispersion levels. The parameter vectors are set to:

$$\text{S1: } (p, q) = (2, 0), \quad (\alpha, \boldsymbol{\beta}, \sigma, \boldsymbol{\phi}) = (0.50, (0.50, 0.20), 0.10, (1.20, -0.30)),$$

S2:  $(p, q) = (2, 0)$ ,  $(\alpha, \beta, \sigma, \phi) = (0.10, (0.50, 0.20), 0.20, (1.20, -0.30))$ ,

S3:  $(p, q) = (1, 1)$ ,  $(\alpha, \beta, \sigma, \phi_1, \theta_1) = (0.40, (0.50, 0.20), 0.10, 0.85, 0.20)$ ,

S4:  $(p, q) = (1, 1)$ ,  $(\alpha, \beta, \sigma, \phi_1, \theta_1) = (0.90, (0.50, 0.20), 0.20, 0.85, 0.20)$ .

Scenarios S1–S2 isolate the effect of dispersion ( $\sigma$ ) under an autoregressive structure, whereas S3–S4 assess the impact of a moving-average component under low/high dispersion. For each scenario, we consider sample sizes  $n \in \{75, 125, 200, 400\}$  and perform  $R$  Monte Carlo replications. In each replication, a burn-in period of length  $B$  is used to mitigate initialization effects, and only the last  $n$  observations are retained for estimation.

## 5.2 Performance measures

For each replication, the parameter vector is estimated by maximizing the conditional log-likelihood  $\ell(\boldsymbol{\vartheta})_{m,n}$  defined in (4.7), with  $\boldsymbol{\vartheta} = (\alpha, \beta^\top, \sigma, \phi^\top, \boldsymbol{\theta}^\top)^\top$ . The recursion for  $q_{\tau,t}$  is computed from (5.1) using the observed past values  $\{Y_{t-i}\}$  and the fitted residuals  $\hat{r}_{t-j}$ , initialized at zero for the first  $m$  observations. Numerical optimization is carried out via BFGS.

Let  $\hat{\psi}^{(r)}$  denote the estimate of a generic parameter  $\psi$  at replication  $r = 1, \dots, R$ , and let  $\psi_0$  be its true value. We compute:

$$\text{RB}(\hat{\psi}) = \frac{\frac{1}{R} \sum_{r=1}^R (\hat{\psi}^{(r)} - \psi_0)}{\psi_0}, \quad (5.4)$$

$$\text{ARB}(\hat{\psi}) = \frac{\frac{1}{R} \sum_{r=1}^R |\hat{\psi}^{(r)} - \psi_0|}{|\psi_0|}, \quad (5.5)$$

$$\text{RMSE}(\hat{\psi}) = \left\{ \frac{1}{R} \sum_{r=1}^R (\hat{\psi}^{(r)} - \psi_0)^2 \right\}^{1/2}. \quad (5.6)$$

These measures are reported for each parameter and  $(n, \text{scenario})$  combination. Algorithm 1 summarizes the simulation and estimation steps.

## 5.3 Results

The Monte Carlo results for the normal kernel at  $\tau = 0.50$  are reported in Tables 1–3. From these tables, we note that, across all scenarios, the estimators exhibit the expected improvement in accuracy as the sample size increases, with systematic reductions in relative bias (RB), absolute relative bias (ARB) and root mean squared error (RMSE) as  $n$  grows.

In scenarios S1 and S2, which correspond to purely autoregressive dynamics, the regression coefficients  $\beta_1$  and  $\beta_2$  display very small relative bias even for the smallest sample size and become essentially unbiased for  $n \geq 200$ . The autoregressive parameters  $\phi_1$  and  $\phi_2$  present moderate negative relative bias in small samples. However, both ARB and RMSE for these parameters decrease markedly as  $n$  increases, indicating consistency of the estimators. The dispersion parameter  $\sigma$  is mildly downward biased in relative terms, but its ARB and RMSE

---

**Algorithm 1** Monte Carlo experiment for the ULS–ARMA model (normal kernel).

---

1. Fix  $\tau \in \{0.25, 0.50, 0.75\}$ , sample sizes  $\mathcal{N} = \{75, 125, 200, 400\}$ , replications  $R$ , burn-in  $B$ , and the set of scenarios  $\{S1, \dots, S4\}$ .
  2. For each scenario  $S \in \{S1, \dots, S4\}$ , each  $n \in \mathcal{N}$ , and each  $\tau$ :
    - (a) For  $r = 1, \dots, R$ :
      - i. Initialize  $Y_1, \dots, Y_m \in (0, 1)$ , set  $\hat{r}_1 = \dots = \hat{r}_m = 0$ , and define  $\mathbf{x}_t = (\cos(2\pi t/12), \sin(2\pi t/12))^\top$ .
      - ii. For  $t = m + 1, \dots, n + B$ :
        - A. Compute  $\eta_t$  from (5.1) using the scenario parameters.
        - B. Set  $q_{\tau,t} = g^{-1}(\eta_t)$  and draw  $Z_t$  from the normal kernel.
        - C. Generate  $Y_t = g^{-1}(\eta_t + \sigma\{Z_t - Q_Z(\tau)\})$  as in (5.3).
        - D. Update  $r_t = g(Y_t) - \eta_t$ .
      - iii. Discard the first  $B$  observations and retain  $Y_{B+1}, \dots, Y_{B+n}$ .
      - iv. Fit the ULS–ARMA model by CML under the normal kernel. Store  $\hat{\boldsymbol{\vartheta}}^{(r)} = (\hat{\alpha}, \hat{\boldsymbol{\beta}}, \hat{\boldsymbol{\phi}}, \hat{\boldsymbol{\theta}}, \hat{\sigma})^\top$ .
    - (b) Compute RB, ARB, and RMSE via (5.4)–(5.6) for all parameters.
- 

remain small throughout, showing stable estimation under both low (S1) and moderate (S2) dispersion levels.

Scenarios S3 and S4 introduce a moving-average component. In these cases, the MA parameter  $\theta_1$  exhibits comparatively large relative bias and ARB for small sample sizes. Nevertheless, both ARB and RMSE for  $\theta_1$  decrease as the sample size increases, suggesting that the estimator is consistent. The autoregressive coefficient  $\phi_1$  and the regression parameters maintain good finite-sample properties, with bias and variability comparable to those observed in scenarios S1–S2. The estimation of the dispersion parameter  $\sigma$  is more sensitive in scenario S3, where the true dispersion is low, but improves substantially in scenario S4 when the true  $\sigma$  is larger.

The RMSE results further corroborate these findings by showing a clear decline as  $n$  increases for all parameters. Overall, the Monte Carlo evidence supports the reliability of the proposed ULS–ARMA estimators across a wide range of dynamic structures and dispersion levels.

Tables 4–5 and Tables 6–7 report the corresponding results for  $\tau = 0.25$  and  $\tau = 0.75$ , respectively. The qualitative behavior of the estimators is broadly consistent with the findings for  $\tau = 0.50$ : bias and variability decrease as  $n$  increases for all parameters, whereas the regression coefficients  $\beta_1$  and  $\beta_2$  remain well-estimated even in small samples. The scale parameter  $\sigma$  tends to display somewhat larger relative bias at  $\tau = 0.25$  compared with  $\tau = 0.75$ , reflecting greater sampling variability in the lower tail of the conditional distribution. In scenarios S3 and S4, the MA coefficient  $\theta_1$  retains its characteristic larger bias in small samples regardless of  $\tau$ , though

the rate of improvement with  $n$  is similar across quantile levels. These results confirm that the finite-sample performance of the CML estimators is robust to the choice of  $\tau$  within the range  $[0.25, 0.75]$ .

**Tab. 1:** Monte Carlo results (normal kernel,  $\tau = 0.50$ ): relative bias (RB) with scenarios S1–S4.

Parameter	S1				S2			
	$n = 75$	$n = 125$	$n = 200$	$n = 400$	$n = 75$	$n = 125$	$n = 200$	$n = 400$
$\alpha$	0.4060	0.1930	0.1144	0.0434	0.3808	0.1985	0.1159	0.0500
$\beta_1$	0.0066	0.0029	-0.0057	0.0002	0.0131	0.0059	-0.0113	0.0004
$\beta_2$	0.0013	0.0178	0.0006	-0.0081	0.0027	0.0355	0.0013	-0.0163
$\phi_1$	-0.0567	-0.0287	-0.0142	-0.0102	-0.0567	-0.0287	-0.0142	-0.0102
$\phi_2$	-0.0904	-0.0506	-0.0189	-0.0266	-0.0904	-0.0506	-0.0189	-0.0266
$\sigma$	-0.0389	-0.0200	-0.0100	-0.0084	-0.0389	-0.0200	-0.0100	-0.0084
Parameter	S3				S4			
	$n = 75$	$n = 125$	$n = 200$	$n = 400$	$n = 75$	$n = 125$	$n = 200$	$n = 400$
$\alpha$	0.3297	0.2550	0.0951	0.0538	0.2268	0.1878	0.0501	0.0290
$\beta_1$	-0.0030	0.0104	-0.0064	-0.0034	-0.0102	0.0087	-0.0190	-0.0072
$\beta_2$	0.0144	-0.0260	-0.0349	0.0044	0.0092	-0.0908	-0.0774	-0.0074
$\phi_1$	-0.0597	-0.0445	-0.0173	-0.0099	-0.0409	-0.0327	-0.0089	-0.0055
$\sigma$	0.9424	0.9670	0.9746	0.9811	0.0111	0.0062	0.0038	0.0328
$\theta_1$	-0.5086	-0.5027	-0.5077	-0.5049	-0.0515	-0.0434	-0.0475	-0.0046

**Tab. 2:** Monte Carlo results (normal kernel,  $\tau = 0.50$ ): absolute relative bias (ARB) with scenarios S1–S4.

Parameter	S1				S2			
	$n = 75$	$n = 125$	$n = 200$	$n = 400$	$n = 75$	$n = 125$	$n = 200$	$n = 400$
$\alpha$	0.5404	0.3151	0.2203	0.1593	0.5469	0.3578	0.2517	0.1862
$\beta_1$	0.0717	0.0618	0.0427	0.0324	0.1433	0.1235	0.0854	0.0649
$\beta_2$	0.1960	0.1325	0.1100	0.0792	0.3920	0.2649	0.2199	0.1584
$\phi_1$	0.0883	0.0647	0.0503	0.0322	0.0883	0.0647	0.0503	0.0322
$\phi_2$	0.3102	0.2323	0.1931	0.1318	0.3102	0.2323	0.1931	0.1318
$\sigma$	0.0697	0.0561	0.0386	0.0306	0.0697	0.0561	0.0386	0.0306
Parameter	S3				S4			
	$n = 75$	$n = 125$	$n = 200$	$n = 400$	$n = 75$	$n = 125$	$n = 200$	$n = 400$
$\alpha$	0.4781	0.3728	0.2352	0.1694	0.4433	0.3464	0.2376	0.1744
$\beta_1$	0.1540	0.1166	0.0900	0.0655	0.2362	0.1869	0.1468	0.1076
$\beta_2$	0.3524	0.2984	0.2380	0.1654	0.4934	0.4261	0.3595	0.2482
$\phi_1$	0.0834	0.0642	0.0408	0.0296	0.0776	0.0608	0.0415	0.0309
$\sigma$	0.9424	0.9670	0.9746	0.9811	0.0793	0.0618	0.0492	0.0541
$\theta_1$	0.5086	0.5027	0.5077	0.5049	0.0996	0.0692	0.0599	0.0599

**Tab. 3:** Monte Carlo results (normal kernel,  $\tau = 0.50$ ): RMSE with scenarios S1–S4.

Parameter	S1				S2			
	$n = 75$	$n = 125$	$n = 200$	$n = 400$	$n = 75$	$n = 125$	$n = 200$	$n = 400$
$\alpha$	0.3576	0.2131	0.1449	0.1020	0.0731	0.0481	0.0329	0.0237
$\beta_1$	0.0446	0.0381	0.0267	0.0203	0.0893	0.0762	0.0534	0.0406
$\beta_2$	0.0484	0.0335	0.0277	0.0196	0.0968	0.0670	0.0553	0.0392
$\phi_1$	0.1360	0.0992	0.0766	0.0497	0.1360	0.0992	0.0766	0.0497
$\phi_2$	0.1167	0.0884	0.0730	0.0495	0.1167	0.0884	0.0730	0.0495
$\sigma$	0.0089	0.0071	0.0047	0.0038	0.0178	0.0142	0.0095	0.0076

Parameter	S3				S4			
	$n = 75$	$n = 125$	$n = 200$	$n = 400$	$n = 75$	$n = 125$	$n = 200$	$n = 400$
$\alpha$	0.2580	0.1998	0.1196	0.0852	0.5473	0.4122	0.2777	0.2080
$\beta_1$	0.0945	0.0725	0.0576	0.0403	0.1449	0.1197	0.0921	0.0702
$\beta_2$	0.0895	0.0730	0.0595	0.0418	0.1247	0.1052	0.0927	0.0662
$\phi_1$	0.0963	0.0730	0.0434	0.0318	0.0913	0.0682	0.0451	0.0344
$\sigma$	0.0958	0.0975	0.0979	0.0984	0.0204	0.0156	0.0128	0.0207
$\theta_1$	0.1045	0.1024	0.1025	0.1016	0.0253	0.0175	0.0148	0.0219

**Tab. 4:** Monte Carlo results (normal kernel,  $\tau = 0.25$ ): relative bias (RB) with scenarios S1–S4.

Parameter	S1				S2			
	$n = 75$	$n = 125$	$n = 200$	$n = 400$	$n = 75$	$n = 125$	$n = 200$	$n = 400$
$\alpha$	0.4664	0.2217	0.1311	0.0503	0.9847	0.4850	0.2834	0.1189
$\beta_1$	0.0066	0.0029	-0.0057	0.0002	0.0131	0.0059	-0.0113	0.0004
$\beta_2$	0.0013	0.0178	0.0006	-0.0081	0.0027	0.0355	0.0012	-0.0163
$\phi_1$	-0.0567	-0.0287	-0.0142	-0.0102	-0.0567	-0.0287	-0.0142	-0.0102
$\phi_2$	-0.0904	-0.0506	-0.0189	-0.0266	-0.0904	-0.0506	-0.0189	-0.0266
$\sigma$	-0.0389	-0.0200	-0.0100	-0.0084	-0.0389	-0.0200	-0.0100	-0.0084

Parameter	S3				S4			
	$n = 75$	$n = 125$	$n = 200$	$n = 400$	$n = 75$	$n = 125$	$n = 200$	$n = 400$
$\alpha$	0.2278	0.1344	-0.0527	-0.1021	0.2581	0.2083	0.0530	0.0319
$\beta_1$	-0.0030	0.0104	-0.0064	-0.0034	0.0010	0.0285	-0.0126	-0.0091
$\beta_2$	0.0144	-0.0260	-0.0349	0.0044	-0.0129	-0.0530	-0.0575	-0.0031
$\phi_1$	-0.0597	-0.0445	-0.0173	-0.0099	-0.0405	-0.0323	-0.0092	-0.0059
$\sigma$	0.9424	0.9670	0.9746	0.9811	0.0052	0.0270	0.0392	0.0289
$\theta_1$	-0.5086	-0.5027	-0.5077	-0.5049	-0.0573	-0.0223	-0.0109	-0.0098

**Tab. 5:** Monte Carlo results (normal kernel,  $\tau = 0.25$ ): RMSE with scenarios S1–S4.

Parameter	S1				S2			
	$n = 75$	$n = 125$	$n = 200$	$n = 400$	$n = 75$	$n = 125$	$n = 200$	$n = 400$
$\alpha$	0.4083	0.2425	0.1650	0.1157	0.1707	0.1046	0.0710	0.0501
$\beta_1$	0.0446	0.0381	0.0267	0.0203	0.0893	0.0762	0.0534	0.0406
$\beta_2$	0.0484	0.0335	0.0277	0.0196	0.0968	0.0670	0.0553	0.0392
$\phi_1$	0.1360	0.0992	0.0766	0.0497	0.1360	0.0992	0.0766	0.0497
$\phi_2$	0.1167	0.0884	0.0730	0.0495	0.1167	0.0884	0.0730	0.0495
$\sigma$	0.0089	0.0071	0.0047	0.0038	0.0178	0.0142	0.0095	0.0076

Parameter	S3				S4			
	$n = 75$	$n = 125$	$n = 200$	$n = 400$	$n = 75$	$n = 125$	$n = 200$	$n = 400$
$\alpha$	0.2744	0.2080	0.1332	0.1044	0.6297	0.4905	0.3317	0.2290
$\beta_1$	0.0945	0.0725	0.0576	0.0403	0.1448	0.1135	0.0945	0.0687
$\beta_2$	0.0895	0.0730	0.0595	0.0418	0.1216	0.1082	0.0879	0.0601
$\phi_1$	0.0963	0.0730	0.0434	0.0318	0.0914	0.0708	0.0469	0.0336
$\sigma$	0.0958	0.0975	0.0979	0.0984	0.0214	0.0220	0.0297	0.0178
$\theta_1$	0.1045	0.1024	0.1025	0.1016	0.0256	0.0251	0.0321	0.0190

**Tab. 6:** Monte Carlo results (normal kernel,  $\tau = 0.75$ ): relative bias (RB) with scenarios S1–S4.

Parameter	S1				S2			
	$n = 75$	$n = 125$	$n = 200$	$n = 400$	$n = 75$	$n = 125$	$n = 200$	$n = 400$
$\alpha$	0.3456	0.1644	0.0976	0.0365	-0.2231	-0.0880	-0.0517	-0.0189
$\beta_1$	0.0066	0.0029	-0.0057	0.0002	0.0131	0.0059	-0.0113	0.0004
$\beta_2$	0.0013	0.0178	0.0006	-0.0081	0.0027	0.0355	0.0012	-0.0163
$\phi_1$	-0.0567	-0.0287	-0.0142	-0.0102	-0.0567	-0.0287	-0.0142	-0.0102
$\phi_2$	-0.0904	-0.0506	-0.0189	-0.0266	-0.0904	-0.0506	-0.0189	-0.0266
$\sigma$	-0.0389	-0.0200	-0.0100	-0.0084	-0.0389	-0.0200	-0.0100	-0.0084

Parameter	S3				S4			
	$n = 75$	$n = 125$	$n = 200$	$n = 400$	$n = 75$	$n = 125$	$n = 200$	$n = 400$
$\alpha$	0.4317	0.3755	0.2430	0.2098	0.1803	0.1803	0.0657	0.0268
$\beta_1$	-0.0019	0.0104	-0.0064	-0.0034	-0.0056	0.0038	-0.0143	-0.0070
$\beta_2$	0.0180	-0.0260	-0.0349	0.0044	-0.0125	-0.0448	-0.0409	0.0059
$\phi_1$	-0.0597	-0.0445	-0.0173	-0.0099	-0.0382	-0.0360	-0.0133	-0.0053
$\sigma$	0.9430	0.9670	0.9746	0.9811	0.0097	0.0217	0.0216	0.0188
$\theta_1$	-0.5091	-0.5027	-0.5077	-0.5049	-0.0489	-0.0290	-0.0262	-0.0191

**Tab. 7:** Monte Carlo results (normal kernel,  $\tau = 0.75$ ): RMSE with scenarios S1–S4.

Parameter	S1				S2			
	$n = 75$	$n = 125$	$n = 200$	$n = 400$	$n = 75$	$n = 125$	$n = 200$	$n = 400$
$\alpha$	0.3069	0.1838	0.1248	0.0884	0.0488	0.0281	0.0210	0.0125
$\beta_1$	0.0446	0.0381	0.0267	0.0203	0.0893	0.0762	0.0534	0.0406
$\beta_2$	0.0484	0.0335	0.0277	0.0196	0.0968	0.0670	0.0553	0.0392
$\phi_1$	0.1360	0.0992	0.0766	0.0497	0.1360	0.0992	0.0766	0.0497
$\phi_2$	0.1167	0.0884	0.0730	0.0495	0.1167	0.0884	0.0730	0.0495
$\sigma$	0.0089	0.0071	0.0047	0.0038	0.0178	0.0142	0.0095	0.0076
Parameter	S3				S4			
	$n = 75$	$n = 125$	$n = 200$	$n = 400$	$n = 75$	$n = 125$	$n = 200$	$n = 400$
$\alpha$	0.2538	0.2076	0.1365	0.1088	0.4617	0.3609	0.2590	0.1570
$\beta_1$	0.0941	0.0725	0.0576	0.0403	0.1457	0.1172	0.0925	0.0678
$\beta_2$	0.0888	0.0730	0.0595	0.0418	0.1286	0.1063	0.0843	0.0633
$\phi_1$	0.0964	0.0730	0.0434	0.0318	0.0902	0.0701	0.0486	0.0313
$\sigma$	0.0958	0.0975	0.0979	0.0984	0.0204	0.0163	0.0131	0.0131
$\theta_1$	0.1046	0.1024	0.1025	0.1016	0.0257	0.0192	0.0157	0.0145

## 6 Application to proportion of stored hydroelectric energy data

This section presents an empirical application of the proposed ULS–ARMA model to a bounded hydrological time series dataset, the monthly proportion of stored hydroelectric energy in the Southeast region of Brazil. The data consist of monthly observations from May 2000 to August 2019, totaling 232 months, and are publicly available at <https://github.com/tatianefribeiro/ubxiiarma>; for more details, the interested reader can see (Ribeiro et al., 2023) and Table 11. The Southeast subsystem plays a central role in the Brazilian interconnected power system and, therefore, monitoring and forecasting stored energy levels is crucial for planning and risk assessment, especially in periods associated with water scarcity and supply stress. We compare the performance of the proposed models with alternative dynamic models for bounded data that have been previously applied to this same series. In particular, we consider the unit Burr XII quantile autoregressive moving average (UBXII–ARMA) model of Ribeiro et al. (2023), the beta autoregressive moving average (betaARMA) introduced by Rocha and Cribari-Neto (2009) within the beta regression framework of Ferrari and Cribari-Neto (2004), and the Kumaraswamy autoregressive moving average (KARMA) model proposed by Bayer et al. (2017). These models represent well-established approaches for modeling and forecasting proportion-valued time series and therefore serve as natural benchmarks for assessing the advantages of the proposed ULS–ARMA specifications.

The series exhibits a pronounced annual seasonal pattern. In order to account for seasonality in a parsimonious way, we follow Ribeiro et al. (2023) and adopt harmonic terms as covariates,

using the trigonometric regressors  $\cos(2\pi t/12)$  and  $\sin(2\pi t/12)$ , as in a simple harmonic regression representation. In addition, in order to capture periods of persistently lower storage levels reported in the literature, we include a crisis indicator (denoted by  $\text{crisis}_t$ ) as an exogenous covariate. Hence, the competing models are fitted under a common regression structure with covariates  $(\cos(2\pi t/12), \sin(2\pi t/12), \text{crisis}_t)$ .

## 6.1 Parameter estimation

Table 8 reports the conditional maximum likelihood estimates and standard errors for all competing specifications, obtained by modeling the conditional median (i.e.,  $\tau = 0.5$ ), which goes in line with previous studies on this same series (Ribeiro et al., 2023). Overall, the results provide strong empirical support for dynamic modeling: in all cases, the autoregressive parameters are highly significant and indicate pronounced persistence in the conditional dynamics of the stored-energy proportion. Across the benchmark specifications, namely UBXII-ARMA, betaAR, and KARMA, an AR(2) structure is selected, with  $\hat{\phi}_1$  ranging from 1.32 to 1.61 and  $\hat{\phi}_2$  between  $-0.41$  and  $-0.67$ , reflecting a highly persistent behavior. A similar AR(2) structure is also selected by the ULS-ARMA model with normal kernel, whose autoregressive coefficients closely match those obtained from the existing unit-valued dynamic models.

In contrast, the ULS-ARMA specification based on the heavier-tailed Student- $t$  kernel leads to a different and more flexible dynamic representation. The Student- $t$  ULS-ARMA model selects an ARMA(1, 1) structure ( $\hat{p} = 3$ ), combining a highly persistent first-order autoregressive component with a statistically significant moving-average term. This indicates that, once robustness to extreme observations is introduced through the Student- $t$  kernel, part of the serial dependence is more effectively captured through short-run innovations rather than additional autoregressive lags.

Regarding the regression component, the estimated covariate effects are remarkably stable across all specifications. In particular, the coefficients associated with the seasonal harmonic terms ( $\beta_1$  and  $\beta_2$ ) are positive and statistically significant at conventional levels for all models, confirming the relevance of seasonal patterns in explaining the conditional quantile dynamics of stored energy. In contrast, the crisis indicator ( $\beta_3$ ) exhibits weaker and less robust effects: it is marginally significant under the UBXII-ARMA model, but becomes statistically insignificant under betaARMA, KARMA, and all ULS-ARMA variants. This finding suggests that, once serial dependence and seasonality are properly accounted for, the remaining impact of the crisis dummy on the conditional median is limited.

In the work of Ribeiro et al. (2023), the UBXII-ARMA model was shown to outperform both the betaARMA model introduced by Rocha and Cribari-Neto (2009) and the KARMA model proposed by Bayer et al. (2017). Motivated by these findings, we conduct a focused comparison between the UBXII-ARMA model and the proposed ULS-ARMA specification with Student- $t$  kernel across a fine grid of quantiles  $\tau \in \{0.01, 0.02, \dots, 0.99\}$ , evaluating model adequacy in terms of log-likelihood and information criteria. In this sense, Table 9 summarizes the averages of the log-likelihood and information criteria computed across the quantile grid. The results show that the ULS-ARMA model with Student- $t$  kernel consistently dominates the UBXII-ARMA

**Tab. 8:** Parameter estimates for the competing models.

Model	Parameter	Estimate	Std. Error	$z$ value	$\Pr(>  z )$
UBXII-ARMA	$\alpha$	0.0206	0.0156	1.3260	0.1848
UBXII-ARMA	$\beta_1$	0.4034	0.0472	8.5449	0.0000
UBXII-ARMA	$\beta_2$	0.1138	0.0419	2.7172	0.0066
UBXII-ARMA	$\beta_3$	-0.2630	0.1316	-1.9988	0.0456
UBXII-ARMA	$\phi_1$	1.3222	0.0432	30.5828	0.0000
UBXII-ARMA	$\phi_2$	-0.4072	0.0430	-9.4752	0.0000
UBXII-ARMA	$c$	11.3464	0.6468	17.5430	0.0000
betaARMA	$\alpha$	0.0071	0.0097	0.7267	0.4674
betaARMA	$\phi_1$	1.3797	0.0504	27.3683	0.0000
betaARMA	$\phi_2$	-0.4170	0.0506	-8.2343	0.0000
betaARMA	$\varphi$	200.7800	19.1045	10.5096	0.0000
betaARMA	$\beta_1$	0.6172	0.0402	15.3585	0.0000
betaARMA	$\beta_2$	0.1791	0.0395	4.5336	0.0000
betaARMA	$\beta_3$	0.0155	0.0948	0.1632	0.8704
KARMA	$\alpha$	0.0304	0.0132	2.3106	0.0209
KARMA	$\phi_1$	1.6120	0.0644	25.0486	0.0000
KARMA	$\phi_2$	-0.6674	0.0621	-10.7487	0.0000
KARMA	$\varphi$	14.6954	0.7177	20.4769	0.0000
KARMA	$\beta_1$	0.8756	0.0637	13.7389	0.0000
KARMA	$\beta_2$	0.3578	0.0869	4.1184	0.0000
KARMA	$\beta_3$	0.0912	0.0746	1.2232	0.2213
ULS-ARMA (Normal)	$\alpha$	0.0073	0.0114	0.6348	0.5256
ULS-ARMA (Normal)	$\beta_1$	0.6181	0.0462	13.3835	0.0000
ULS-ARMA (Normal)	$\beta_2$	0.1910	0.0462	4.1333	0.0000
ULS-ARMA (Normal)	$\beta_3$	0.0255	0.1105	0.2306	0.8176
ULS-ARMA (Normal)	$\phi_1$	1.3823	0.0626	22.0645	0.0000
ULS-ARMA (Normal)	$\phi_2$	-0.4158	0.0622	-6.6890	0.0000
ULS-ARMA (Normal)	$\sigma$	0.1604	0.0076	20.9762	0.0000
ULS-ARMA ( $t$ )	$\alpha$	-0.0133	0.0138	-0.9621	0.3360
ULS-ARMA ( $t$ )	$\beta_1$	0.5535	0.0356	15.5379	0.0000
ULS-ARMA ( $t$ )	$\beta_2$	0.1900	0.0340	5.5902	0.0000
ULS-ARMA ( $t$ )	$\beta_3$	0.1406	0.1163	1.2086	0.2268
ULS-ARMA ( $t$ )	$\phi_1$	0.9539	0.0148	64.5236	0.0000
ULS-ARMA ( $t$ )	$\theta_1$	0.0591	0.0082	7.2280	0.0000
ULS-ARMA ( $t$ )	$\sigma$	0.1076	0.0072	14.8435	0.0000

model, yielding a substantially higher average log-likelihood and uniformly lower AIC, BIC, CAIC, and HQIC values. These findings indicate that the gains achieved by the proposed model are not restricted to a specific quantile level, but rather persist across the entire conditional distribution, highlighting the benefits of combining quantile-based dynamics with a flexible unit-log-symmetric distribution capable of accommodating heavier tails.

**Tab. 9:** Averages of the log-likelihood and information criteria computed across  $\tau \in \{0.01, 0.02, \dots, 0.99\}$  for the competing quantile-based models.

Indicator	UBXII-ARMA	ULS-ARMA (Student- $t$ )
log-likelihood	410.168	444.331
AIC	-806.013	-873.953
BIC	-781.645	-848.927
CAIC	-806.013	-873.953
HQIC	-808.256	-876.256

## 6.2 Out-of-sample forecasting performance

In order to evaluate predictive accuracy, we computed out-of-sample forecast errors for horizons  $h = 1, \dots, 10$  using the mean squared error (MSE) and mean absolute percentage error (MAPE). Results are summarized in Tab. 10. For very short horizons ( $h = 1$  and  $h = 2$ ), KARMA(2) achieves the smallest MSE and MAPE; however, its performance deteriorates drastically for  $h \geq 3$ , producing extremely large errors relative to all other models. This indicates that, although KARMA(2) may fit local one-step variation, it does not provide stable multi-step dynamics for this dataset. In contrast, the ULS-ARMA model with Student- $t$  kernel delivers the most consistent multi-step forecasting performance. From  $h = 3$  onward, the Student- $t$  ULS-ARMA attains the lowest MSE for all horizons  $h = 3, \dots, 10$ , and simultaneously yields the smallest MAPE in the same range (Tab. 10). In practical terms, this means that the ULS-ARMA specification provides superior medium- and long-horizon predictions for the stored-energy proportion, which is particularly relevant for operational planning contexts where decision-making often relies on forecasts beyond one or two periods ahead.

The UBXII-AR(2), betaARMA(2), and the Normal ULS-ARMA alternative show intermediate performance: they remain stable across horizons but are consistently dominated by the Student- $t$  ULS-ARMA for  $h \geq 3$ . This suggests that allowing heavier tails via the Student- $t$  kernel is beneficial for capturing occasional atypical movements in the stored-energy proportion, improving the robustness of the conditional quantile recursion and reducing forecast error accumulation.

In summary, the application confirms that dynamic unit-log-symmetric modeling is well-suited for bounded energy storage proportions. The fitted models capture strong serial persistence and meaningful covariate effects in the conditional quantile. Among all competitors, the Student- $t$  ULS-ARMA specification stands out as the most reliable approach for multi-step forecasting, achieving the best overall out-of-sample performance for horizons  $h = 3$  to  $h = 10$  (Tab. 10). These results support the usefulness of combining quantile-based dynamics with a flexible unit-log-symmetric distributional structure.

**Tab. 10:** Out-of-sample forecast errors for prediction horizons  $h = 1, \dots, 10$ .

Model	Forecast horizon $h$									
	$h = 1$	$h = 2$	$h = 3$	$h = 4$	$h = 5$	$h = 6$	$h = 7$	$h = 8$	$h = 9$	$h = 10$
<b>(a) Mean Squared Error (MSE)</b>										
UBXII-ARMA(2)	0.0008	0.0008	0.0010	0.0026	0.0025	0.0024	0.0022	0.0020	0.0018	0.0017
betaARMA(2)	0.0011	0.0010	0.0013	0.0038	0.0045	0.0050	0.0053	0.0049	0.0044	0.0039
KAR(2)	<b>0.0005</b>	<b>0.0003</b>	0.0063	0.0221	0.0345	0.0456	0.0540	0.0586	0.0598	0.0586
ULS-ARMA (Normal)	0.0011	0.0011	0.0013	0.0036	0.0042	0.0047	0.0049	0.0046	0.0041	0.0037
ULS-ARMA (t)	0.0014	0.0017	<b>0.0012</b>	<b>0.0018</b>	<b>0.0016</b>	<b>0.0014</b>	<b>0.0012</b>	<b>0.0011</b>	<b>0.0012</b>	<b>0.0015</b>
<b>(b) Mean Absolute Percentage Error (MAPE)</b>										
UBXII-ARMA(2)	11.88	10.76	12.04	16.23	15.28	14.29	13.45	12.44	11.43	10.96
betaARMA(2)	13.52	12.20	13.68	19.34	19.69	19.67	19.31	18.22	16.51	14.97
KAR(2)	<b>9.46</b>	<b>6.11</b>	20.88	38.08	44.97	49.22	51.99	53.46	54.01	54.16
ULS-ARMA (Normal)	13.91	12.80	13.65	18.97	19.19	19.15	18.81	17.75	16.06	14.61
ULS-ARMA (t)	15.56	15.82	<b>12.52</b>	<b>14.61</b>	<b>12.96</b>	<b>11.64</b>	<b>10.39</b>	<b>9.50</b>	<b>9.62</b>	<b>10.13</b>

### 6.3 Residual analysis

In order to evaluate the adequacy of the fitted ULS-ARMA models, we carry out a residual analysis based on two complementary diagnostics: the generalized Cox-Snell residuals and the randomized quantile residuals. These tools allow us to assess whether the assumed conditional distributions are consistent with the observed data, and whether any systematic departure from the fitted model remains unexplained.

Let  $\hat{q}_{\tau,t}$  denote the fitted conditional  $\tau$ -quantile at time  $t$  and let  $\hat{\sigma}$  denote the estimated scale parameter. The generalized Cox-Snell (GCS) residual is defined as

$$r_{\text{CS},t} = -\log\left(1 - F_t(y_t)\right), \quad (6.1)$$

where  $F_t(y_t) = F_{Y_t|\mathcal{A}_{t-1}}(y_t; \hat{q}_{\tau,t}, \hat{\sigma})$  is the fitted conditional CDF of  $Y_t$  evaluated at the observed value  $y_t$ . Under a correctly specified model,  $r_{\text{CS},t}$  follows approximately an  $\text{Exp}(1)$  distribution, so that a QQ plot of the GCS residuals against  $\text{Exp}(1)$  quantiles provides a visual check of distributional adequacy.

The randomized quantile (RQ) residual is defined as

$$r_{\text{q},t} = \Phi^{-1}\left(F_t(y_t)\right), \quad (6.2)$$

where  $\Phi^{-1}(\cdot)$  denotes the standard normal quantile function. Under a correctly specified model,  $r_{\text{q},t}$  follows a standard normal distribution, whereas systematic departures from normality in a QQ plot of  $r_{\text{q},t}$  against  $N(0, 1)$  quantiles indicate model misspecification.

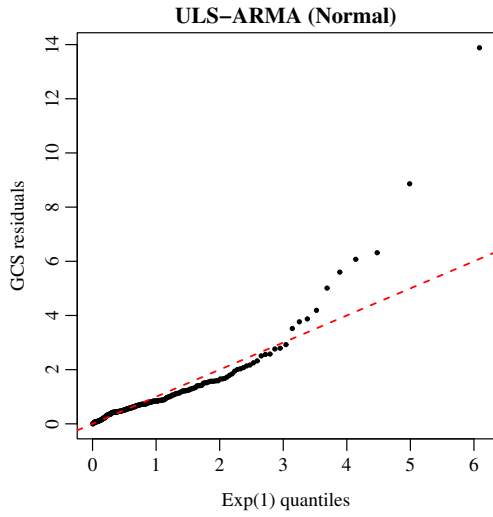
Figure 1 displays the QQ plots of both residual types for the two ULS–ARMA specifications, namely the model with normal kernel (AR(2) structure) and the model with Student- $t$  kernel (ARMA(1,1),  $\hat{\nu} = 3$ ). For the GCS residuals (panels (a) and (c)), the points align closely with the Exp(1) reference line in both cases, indicating that the fitted conditional distributions provide an adequate description of the observed proportions. For the RQ residuals (panels (b) and (d)), the Student- $t$  specification exhibits a slightly tighter adherence to the  $N(0, 1)$  reference line, in particular in the tails, which is consistent with the superior predictive performance documented in Section 6.2. Overall, the residual analysis supports the adequacy of both ULS–ARMA specifications and confirms that the conditional distribution is well-calibrated, with a marginal advantage for the heavy-tailed formulation.

## 7 Concluding remarks

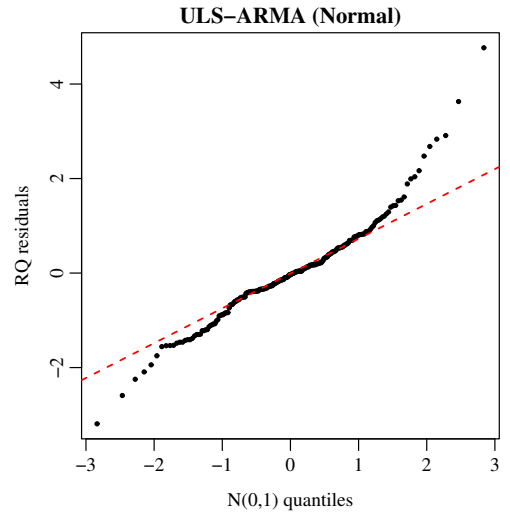
It is widely known that bounded time series data, such as proportions and rates, arise frequently in environmental, economic, and hydrological applications and require dedicated distributional and inferential frameworks. In this paper, we proposed the quantile unit-log-symmetric autoregressive moving average (QULS–ARMA) model for bounded time series. The model extends the unit-log-symmetric distribution to a dynamic setting by introducing ARMA-type dependence directly in the conditional quantile, allowing for flexible distributional shapes through the normal and Student- $t$  log-symmetric kernels. This construction provides a framework for proportion data arising from ratios of dependent positive components, whereas serial dependence and asymmetric dynamics are explicitly accommodated through the ARMA quantile structure. Theoretical formulation and conditional maximum likelihood estimation were developed under a quantile parameterization, and Monte Carlo simulation studies showed good finite-sample performance of the proposed estimators across a range of scenarios, quantile levels  $\tau \in \{0.25, 0.50, 0.75\}$ , and kernel specifications. The residual analysis based on generalized Cox–Snell and randomized quantile residuals confirmed the adequacy of the fitted conditional distributions. An empirical application to monthly proportions of stored hydroelectric energy in Brazil illustrated the practical relevance of the proposed model. The proposed ULS–ARMA specification, especially under the Student- $t$  kernel, provided superior multi-step forecasting performance when compared with established competitors. Extensions to multivariate bounded time series and seasonal autoregressive moving average models are currently under investigation.

**Acknowledgments** This study was financed in part by the Coordenação de Aperfeiçoamento de Pessoal de Nível Superior - Brasil (CAPES) (Finance Code 001). Roberto Vila and Helton Saulo gratefully acknowledge financial support from FAP-DF and CNPq, Brazil.

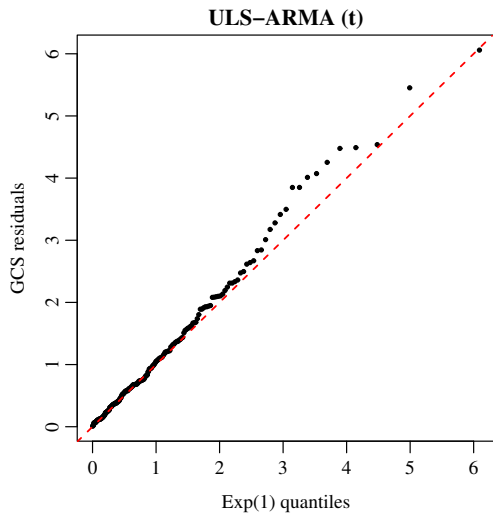
**Disclosure statement** There are no conflicts of interest to disclose.



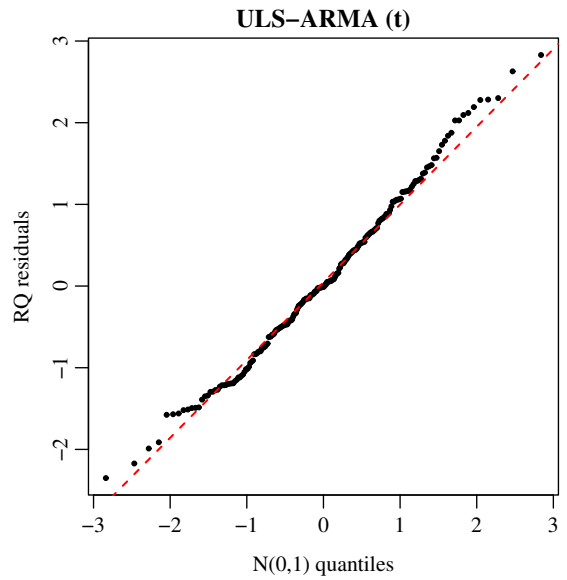
(a) GCS residuals, ULS-ARMA (Normal)



(b) RQ residuals, ULS-ARMA (Normal)



(c) GCS residuals, ULS-ARMA ( $t$ )



(d) RQ residuals, ULS-ARMA ( $t$ )

**Fig. 1:** QQ plots of the generalized Cox–Snell residuals (left panels) and the randomized quantile residuals (right panels) for the ULS–ARMA model with normal kernel (AR(2), top row) and Student- $t$  kernel (ARMA(1, 1),  $\hat{\nu} = 3$ , bottom row).

## References

Andersen, B. A. (1970). Asymptotic properties of conditional maximum-likelihood estimators. *Journal of the Royal Statistic Society Serie B*, 32:283–301.

**Tab. 11:** Monthly proportion of stored hydroelectric energy in the Southeast region of Brazil.

Year	Jan	Feb	Mar	Apr	May	Jun	Jul	Aug	Sep	Oct	Nov	Dec
2000					0.536800	0.471400	0.399200	0.322700	0.308400	0.230500	0.222100	0.286700
2001	0.315600	0.335900	0.346800	0.323000	0.298800	0.287100	0.268500	0.234600	0.206900	0.211300	0.231900	0.325300
2002	0.470600	0.633300	0.703700	0.692300	0.674700	0.648200	0.596000	0.536200	0.491500	0.409600	0.384400	0.414100
2003	0.588000	0.679600	0.744100	0.776200	0.761400	0.728800	0.673200	0.591200	0.501000	0.407800	0.360000	0.373400
2004	0.473600	0.664600	0.759200	0.807800	0.826800	0.822500	0.803300	0.745000	0.659200	0.617900	0.593000	0.645400
2005	0.757600	0.787400	0.859100	0.857400	0.853400	0.825600	0.781600	0.700600	0.652700	0.603500	0.592200	0.671000
2006	0.711400	0.784600	0.853300	0.873200	0.846700	0.783000	0.701300	0.593800	0.503400	0.456300	0.428000	0.536600
2007	0.785500	0.846100	0.873300	0.878100	0.867700	0.831800	0.795200	0.720100	0.620300	0.516100	0.481800	0.461200
2008	0.507700	0.655800	0.785000	0.822400	0.829000	0.795500	0.731500	0.664000	0.578500	0.519100	0.497300	0.558200
2009	0.661100	0.760700	0.805800	0.835500	0.821900	0.785700	0.761000	0.724800	0.702200	0.691200	0.673100	0.723000
2010	0.766900	0.778400	0.825100	0.818100	0.786400	0.743500	0.678800	0.585500	0.492500	0.431000	0.406400	0.447700
2011	0.629900	0.681200	0.829200	0.878000	0.878200	0.852700	0.806200	0.740700	0.653400	0.613700	0.570300	0.606400
2012	0.760700	0.800100	0.784800	0.760400	0.724100	0.724300	0.668900	0.575100	0.478900	0.370200	0.318900	0.288600
2013	0.374700	0.456000	0.541600	0.625500	0.627500	0.637700	0.608600	0.551300	0.486900	0.450700	0.416300	0.430100
2014	0.401700	0.347300	0.363500	0.380300	0.373400	0.364300	0.343200	0.303100	0.251700	0.187400	0.158200	0.193100
2015	0.170400	0.206900	0.285400	0.335800	0.360600	0.361500	0.374200	0.342900	0.322800	0.277400	0.275000	0.297900
2016	0.444300	0.509300	0.582800	0.577100	0.568500	0.561400	0.515900	0.459400	0.401600	0.348300	0.334700	0.337400
2017	0.373300	0.403800	0.414500	0.418600	0.433200	0.421200	0.381600	0.325000	0.242100	0.176100	0.187400	0.226000
2018	0.311333	0.368382	0.423658	0.439873	0.425606	0.397108	0.342491	0.279828	0.229317	0.202239		

Bayer, F. M., Bayer, D. M., and Pumi, G. (2017). Kumaraswamy autoregressive moving average models for double bounded environmental data. *Journal of Hydrology*, 555:385–396.

Ferrari, S. and Cribari-Neto, F. (2004). Beta regression for modelling rates and proportions. *Journal of Applied Statistics*, 31:799–815.

Koenker, R. and Xiao, Z. (2006). Quantile autoregression. *Journal of the American Statistical Association*, 101:980–990.

Kumaraswamy, P. (1980). A generalized probability density function for double-bounded random processes. *Journal of Hydrology*, 46:79–88.

Lucas, A. (1997). Robustness of the Student- $t$  based m-estimator. *Communications in Statistics: Theory and Methods*, 41:1165–1182.

Ribeiro, T. F., Peña Ramírez, F. A., Guerra, R. R., Alencar, A. P., and Cordeiro, G. M. (2023). Forecasting the proportion of stored energy using the unit burr xii quantile autoregressive moving average model. *Computational and Applied Mathematics*, 43:27.

Rocha, A. V. and Cribari-Neto, F. (2009). Beta autoregressive moving average models. *TEST*, 18(3):529–545.

Vanegas, L. H. and Paula, G. A. (2016). Log-symmetric distributions: statistical properties and parameter estimation. *Brazilian Journal of Probability and Statistics*, 30:196–220.

Vila, R., Balakrishnan, N., Saulo, H., and Protazio, A. (2023). Bivariate log-symmetric models: distributional properties, parameter estimation and an application to public spending data. *Brazilian Journal of Probability and Statistics*, 37:619–642.

Vila, R., Balakrishnan, N., Saulo, H., and Zörnig, P. (2024). Unit-log-symmetric models: characterization, statistical properties and their applications to analyzing an internet access data. *Quality & Quantity*, 58(5):4779–4806.